

Cryogenic 2 mm wave electron spin resonance spectrometer with application to atomic hydrogen gas below 100 mK

Sergei Vasilyev^{a)} and Jarno Järvinen

Wihuri Physical Laboratory, Department of Physics, University of Turku, 20014 Turku, Finland

Esa Tjukanoff

Department of Information Technology, University of Turku, 20014 Turku, Finland

Alexander Kharitonov

RRC Kurchatov Institute, 123182 Moscow, Russia

Simo Jaakkola

Wihuri Physical Laboratory, Department of Physics, University of Turku, 20014 Turku, Finland

(Received 14 August 2003; accepted 14 October 2003)

We describe a 128 GHz electron-spin-resonance spectrometer based on heterodyne detection with double frequency conversion utilizing cryogenic Schottky-diode mixers. Together with other mm-wave components installed into a dilution refrigerator cryostat, the mixers comprise a bridge operating at 1.5 K. A miniature Fabry–Perot resonator is used to detect samples of bulk and surface-adsorbed atomic hydrogen gas at temperatures below 100 mK. The sensitivity is 2×10^9 spins/Gauss at the excitation power of 20 pW. © 2004 American Institute of Physics.
[DOI: 10.1063/1.1633006]

I. INTRODUCTION

Sensitivity of an electron-spin-resonance (ESR) spectrometer increases at higher operating frequencies basically because of larger microwave quanta absorbed in the resonance. Higher frequencies correspond to higher magnetic fields resulting also in a better resolution due to larger Zeeman splittings of the hyperfine levels. In the case of spin-polarized atomic hydrogen gas ($H\downarrow$) magnetic fields of several tesla are also required to increase the stability of the samples. This predetermines the operating frequency to the mm-wave range.^{1–4} A specific feature of ESR on $H\downarrow$ is the resonance-induced destruction of the sample. Atoms with flipped spins promptly recombine in collisions with other atoms.⁵ This means that the resonance power destroys twice as many atoms as mm-wave quanta absorbed. To decrease the ESR destruction, one has to use excitation power in the picowatt region. The conventional method of magnetic field modulation to increase sensitivity cannot be used at low temperatures because of eddy current heating and shielding of the modulation field. Therefore, the choice of the spectrometer scheme becomes of prime importance to ensure a high sensitivity at low excitation powers.

InSb hot electron detectors are often used in the mm-wave ESR spectroscopy and radio astronomy for detecting weak signals. When cooled to liquid-helium temperatures InSb detectors have high sensitivity and low noise. However, their modulation frequency is limited to ≤ 10 MHz which is too low to be used in the heterodyne detection scheme because it is difficult to filter the sidebands differing so little in frequency. Therefore, homodyne detection with mm-wave power modulation was utilized in the previous version of our

ESR spectrometer.³ Its main disadvantages were a relatively large low-frequency noise and drifts due to the general $1/f$ dependence. Cryogenic mixers developed in radio astronomy are good alternatives to InSb detectors. Effective noise temperatures ≤ 300 K have been reported for Schottky barrier diodes^{6,7} and even ≤ 100 K for superconductor–insulator–superconductor (SIS) type diodes.⁸ Statt *et al.*² used a heterodyne spectrometer utilizing a Schottky mixer operating at room temperature for studies of $H\downarrow$. A relatively high mixer noise temperature, about 650 K, and high losses of mm-wave power between the resonator and the detector were the main limitations of their spectrometer. Another difficulty, typically met in the mm-wave range, was to adjust the coupling of the ESR resonator to the transmission line and to control it after cooling the resonator to subkelvin temperatures. An improper coupling leads to a large signal reflected from the resonator. This creates extra noise and limits the rf gain and the dynamic reserve of the detection system.

In the spectrometer described here, we implemented heterodyne detection with double frequency conversion (Fig. 1). The lock-in amplifier used at the final stage of signal processing sets the upper limit of the first intermediate frequency (IF) to $f_1 \leq 200$ MHz which is yet too low for a proper filtering in the 130 GHz range and, therefore, we have to use a second IF at $f_2 \approx 1.15$ GHz. Another mm-wave source is not needed because we use single side band (SSB) generation techniques mixing f_2 with the main mm-wave frequency f_0 followed by a bandpass filter. Correspondingly, the signal reflected from the ESR resonator is downconverted twice and finally processed by the rf lock in giving the absorption and dispersion ESR signals simultaneously. A novel feature of our apparatus is a fully cryogenic mm-wave bridge including Schottky mixers for up- and downconvert-

^{a)}Electronic mail: servas@utu.fi

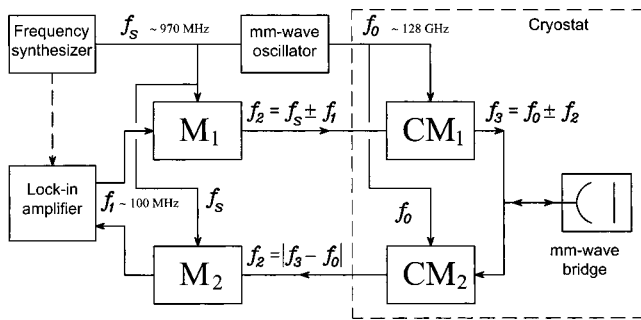


FIG. 1. Block diagram of the ESR spectrometer. M_1 and M_2 are room-temperature mixers used in the first frequency conversion stage. CM_1 and CM_2 are cryogenic mm-wave mixers operating at 1.5 K. All frequencies can be locked to a single reference, e.g., the clock of the frequency synthesizer.

ers and using the bridge compensation principle to reduce the constant off-resonance mm-wave signal reflected from the resonator. We achieve a sensitivity of $\approx 2 \times 10^9$ spins/Gauss at a 20 pW mm-wave excitation power.

II. ROOM-TEMPERATURE COMPONENTS

A schematic diagram of the spectrometer is shown in Fig. 2. The mm-wave source is a Gunn diode oscillator (Millitech GDV-19-5-15) operating at the frequency range of 41–44 GHz. It is phase locked to a HP8656B frequency synthesizer, which provides an output in the range of f_s

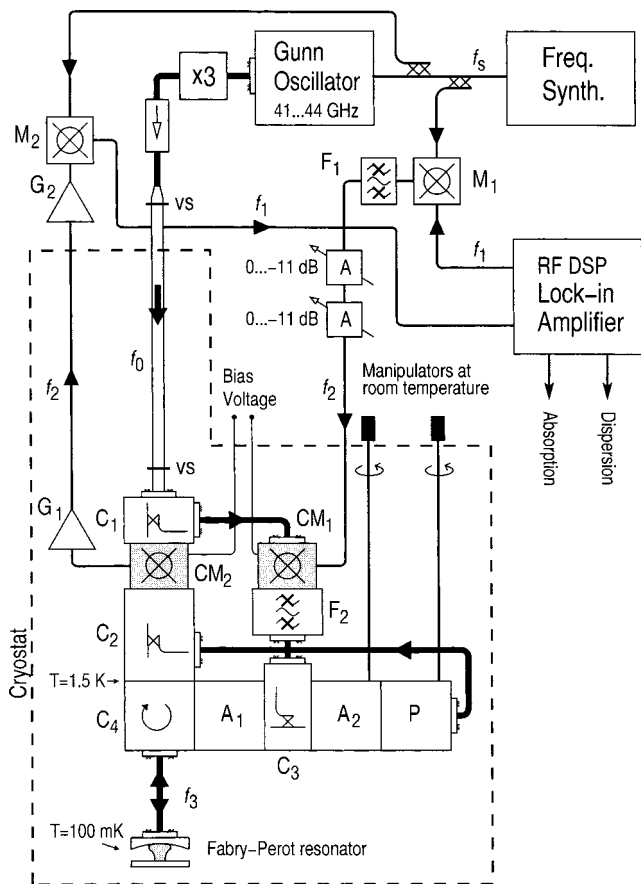


FIG. 2. Schematic diagram of the spectrometer: A = attenuator, C = power splitter/directional coupler, F = filter, G = amplifier, M = microwave mixer, and CM = cryogenic mm-wave mixer.

= 922–998 MHz derived from its internal 10 MHz clock. The Gunn frequency is tripled (Millitech FTT-08) to the range of $f_0 = 123–132$ GHz.

The mm-wave power of 1 mW is delivered to the low-temperature part of the spectrometer through a 1.5 m long 7.2×3.4 mm oversized waveguide. The power loss is 5 dB depending slightly on frequency. The waveguide goes through the main He bath of the cryostat into the vacuum can of the dilution refrigerator and has two vacuum seals, one at the entrance to the main helium bath and the other seals the vacuum can from the helium bath. The seals are made by epoxying a 25 μ m Kapton film across the waveguide connection flanges. To ensure sufficient thermal insulation, a 40 cm long section of the waveguide above the maximum helium level is made of Cu-plated CuNi.

The first IF (f_1) is taken from the internal reference oscillator of a Stanford Research Systems SR844 RF lock-in amplifier. The second IF (f_2) is obtained by mixing f_s with f_1 at mixer M_1 (Mini-Circuits ZFL-2) and filtering one of the sidebands $f_2 = f_s \pm f_1$ with the bandpass filter F_1 . The sideband was selected to get the best signal-to-noise ratio. The power level of the second IF is adjusted by two HP8494A calibrated attenuators.

The ESR signal power at f_2 going out of the cryostat is amplified by a 28 dB low noise amplifier G_2 (Mini-Circuits ZHL-0812 MLN) and downconverted to f_1 at mixer M_2 (Mini-Circuits ZFL-2). Finally, the signal is processed by the rf lock-in amplifier which provides absorption and dispersion line shapes simultaneously and stores them to a computer. All of the rf and dc voltages were fed in and out of the cryostat by low-temperature CuNi coaxial cables.

III. CRYOGENIC COMPONENTS

The main part of the spectrometer is the cryogenic mm-wave bridge (Fig. 1) based on two identical balanced mixers CM_1 and CM_2 . The former works as a sideband generator and creates an excitation signal $f_3 = f_0 \pm f_2$ to the ESR resonator. The latter works as the mm-wave detector of the bridge. It converts the signal reflected from the resonator down to the frequency f_2 preserving both amplitude and phase information. The mixers are similar to those described in Ref. 9, utilizing GaAs Schottky diodes.¹⁰ Figure 3 shows some current–voltage (I – V) curves of the mixers. The optimal dc bias was found to be about 150 μ A for CM_1 and about 1 mA for CM_2 . This leads to dc heating of less than 2 mW, well below the cooling power of the 1 K plate of the dilution refrigerator. The SSB conversion loss of the sideband generator was about 15 dB. It is known that more than 1 mW of local oscillator (LO) power is required for such type of mixers to achieve the minimal (saturated) conversion loss. However, the loss is not important for the sideband generator, because we are not interested in high excitation powers. Yet, for the mixer CM_2 the LO power should be optimized to get the highest sensitivity. Unfortunately, the maximum LO power of about 200 μ W available at the input of CM_2 is far too small for saturation of the conversion loss. In Fig. 4, we present the dependence of the conversion loss of the main mixer on the LO power. The loss slightly de-

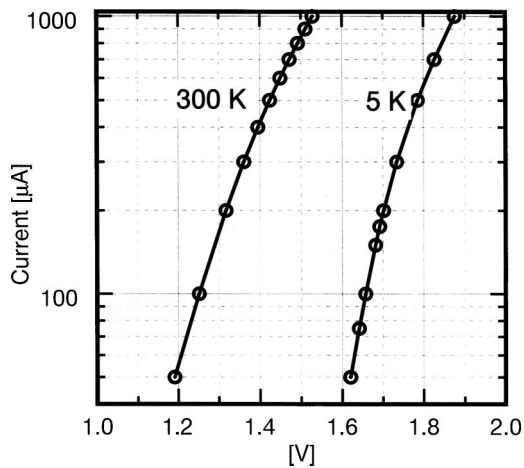


FIG. 3. I - V curves of the AA138B3 mm-wave mixer diodes at room temperature and 5 K.

creases when the mixer is cooled to low temperatures. To prevent a possible interference through the dc bias of the mixers we installed miniature LCR low pass filters to the terminals of the mixers.

The millimeter-wave power (f_0) entering the cryogenic bridge is split into two parts by the directional coupler C_1 . Most of the power (-0.7 dB) goes to CM_2 providing the LO power and a smaller fraction (-13 dB) to the sideband generator CM_1 where it is mixed with the second IF (f_2). The sideband $f_3 = f_0 \pm f_2$ is selected by filter F_2 . Different filters can be used to select the upper or lower sideband and thus the ESR excitation frequency f_3 . The filters are of fin-line type¹¹ with a typical frequency response illustrated in Fig. 5. The maximum generated SSB power at CM_1 is about $1 \mu\text{W}$. After the filter a power splitter C_3 directs the mm-wave energy into the two arms of the mm-wave bridge. A -4.5 dB fraction goes to the main arm, passes the attenuator A_1 , and enters the resonator through the circulator C_4 .¹² The attenuator A_1 adjusts the ESR excitation power. However, we found it more convenient to do the adjustment by changing the power of the second IF at room temperature. ESR in the sample modulates the reflection coefficient of the resonator and encodes the absorption and dispersion signals into the reflected wave. The compensating arm of the mm-wave bridge contains a tunable attenuator A_2 and a phase shifter P

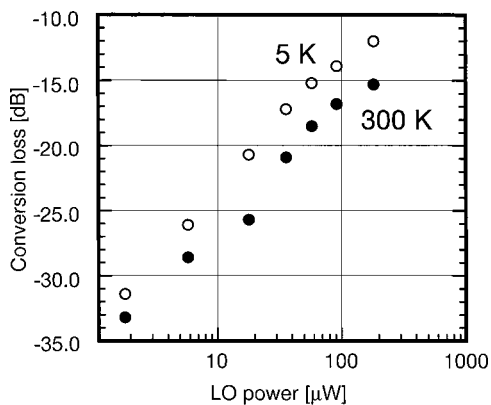


FIG. 4. Conversion loss of the main mixer CM_2 as a function of LO power at room temperature and at 5 K. Optimum dc bias of $I = 1$ mA was used.

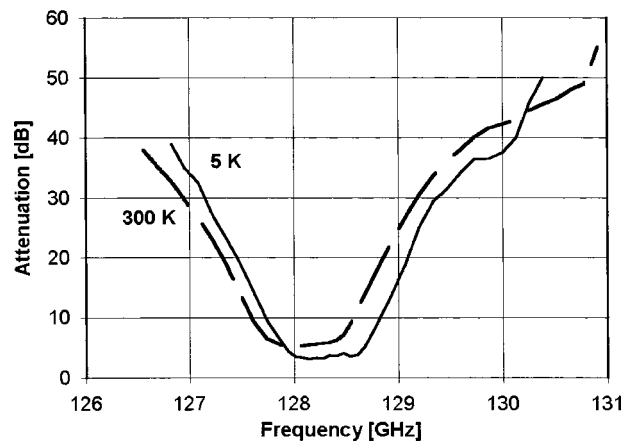


FIG. 5. 128 GHz bandpass filter frequency response at room temperature and at 5 K.

controlled mechanically from the top of the cryostat with high-vacuum rotational manipulators connected to A_2 and P by 1.5 m long 1 mm diameter stainless-steel capillaries. The amplitude and phase of the mm wave in the compensating arm are adjusted so that the sum of the off-resonance waves at the CM_1 input is close to zero.

The ESR resonator is located in the center of a superconducting magnet and is connected to the mm-wave bridge with a 25 cm long standard D -band waveguide. A 10 cm piece of thin-walled (0.2 mm) CuNi waveguide is installed to ensure thermal insulation. The total loss of the mm-wave signal from the resonator to the main mixer is about 4 dB. The maximum power incident to the ESR resonator is of the order of $0.1 \mu\text{W}$. A homemade low noise field-effect transistor (FET) preamplifier G_1 is located near CM_2 to increase the signal level in the long CuNi coaxial cable going out of the cryostat. The preamplifier has a gain of 18 dB and it releases about 15 mW of heat which is too much for the 1 K plate of the dilution refrigerator. Therefore, the preamplifier operates at 4.2 K and is thermally insulated from the mm-wave bridge by a 10 cm piece of CuNi coaxial cable.

The components of the cryogenic mm-wave bridge are assembled into a $15 \times 12 \times 2$ cm block mounted inside the vacuum can of the dilution refrigerator in a space between the mixing chamber and continuous heat exchangers (Fig. 6). The bridge is located 10–20 cm above the top of the magnet where the fringing field of 0.1–0.05 T does not influence the bridge operation. The spectrometer components produce no significant heat load to the refrigerator. The minimum temperature of the sample cell was limited to 30 mK by the heat load from the components of the H_{\downarrow} setup.

To detect ESR in our experiments with two-dimensional (2D) atomic hydrogen,¹³ we used a semi-confocal Fabry–Perot resonator operating in the TEM_{002} mode. It is made of a hemispherical ($R = 6.5$ mm) mirror and a flat mirror. The 1.5 mm diameter central part of the flat mirror can be cooled to temperatures substantially lower than the rest of the sample cell, providing thermal compression of 2D H_{\downarrow} .¹³ The loaded Q of the resonator is about 2700. The effective volume of the bulk gas in the resonator is $1.3 \times 10^{-3} \text{ cm}^3$ and the effective area of the 2D gas is $1.4 \times 10^{-2} \text{ cm}^2$. The resonator is coupled to the waveguide through a circular 0.5 mm

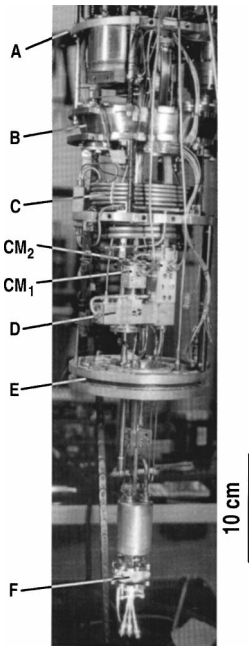


FIG. 6. Photograph of the dilution refrigerator with the cryogenic ESR bridge: A=1 K plate, B=still, C=continuous heat exchangers, CM = cryogenic mm-wave mixer, D=mm-wave bridge, E= $^3\text{He}/^4\text{He}$ mixing chamber, and F=sample cell with Fabry–Perot resonator.

diameter iris in the center of the hemispherical mirror. The resonator is substantially undercoupled when cooled to the operating temperature.

A resonant magnetic field of about 4.6 T is generated by a 7 cm bore superconducting solenoid (Cryomagnetics Inc.) operating in persistent mode. A sweep coil is mounted in the bore of the main magnet. The maximum sweep rate is limited to about 1 mT/s by the eddy current heating of the sample cell at 100 mK. The specified inhomogeneity of the main magnet at its center is less than 10 ppm/cm (0.05 mT/cm) and the field decay rate is $2 \times 10^{-9} \text{ s}^{-1}$. However, the presence of weakly magnetic brass components of the sample cell in the vicinity of the resonator increased the inhomogeneity to about 1 mT/cm. The axial homogeneity was improved with special Maxwell gradient coils wound on the still radiation shield of the dilution refrigerator. By optimizing the current in the gradient coils, we succeeded in decreasing the width of the ESR signal from the bulk hydrogen gas down to 0.25 mT/cm.

IV. TUNING UP THE SPECTROMETER

The main difficulty in setting up and tuning the spectrometer arises from the changes in the component properties during the cooldown. To measure these changes, we have tested each component separately at 4.2 K as demonstrated in Figs. 3–5. The choice of the operating frequency is determined first by the operating range of the Gunn oscillator and by the low-temperature circulator C_4 ($f = 128 \pm 1$ GHz). Then, the frequency tuning range is determined by the filter F_2 , whose bandwidth is narrowest. Several mm-wave filters were manufactured and, by choosing an appropriate one, we could cover the whole 128 ± 1 GHz band of the circulator C_4 . The ESR resonator frequency f_r has also been set to be

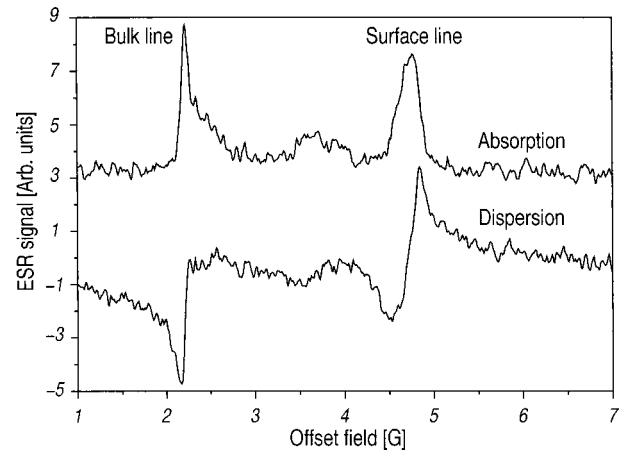


FIG. 7. Example of the $\text{H}\downarrow$ spectrum recorded at a 20 pW mm-wave excitation power and a lock-in time constant of 0.1 s. Density of $\text{H}\downarrow$ atoms in the bulk gas was $2.1 \times 10^{13} \text{ cm}^{-3}$ and on the surface $2.5 \times 10^{12} \text{ cm}^{-2}$. Corresponding temperatures the bulk and surface samples were 120 mK and 93 mK.

within this band. During the cooldown, f_r increases by about 0.2 GHz, and to track this change the spectrometer can be fine tuned by varying f_s or f_1 . We use a HP8753D network analyzer to measure S_{21} by connecting its excitation port to the IF input at the cryostat and the detection port to the output of the amplifier G_2 . Once the sample cell and the spectrometer are cooled to the desired temperatures, the balancing of the mm-wave bridge is carried out by keeping the magnetic field off resonance and minimizing the signal detected by the lock-in amplifier with the help of the attenuator A_2 and the phase shifter P. In this way, we could reduce the reflected signal by more than 30 dB. The remaining signal was still about 30 dB above the noise level. Further improvement of the balance was difficult because of the nonideal properties of the attenuator and the phase shifter. Changing the amplitude of the mm-wave with A_2 also slightly affects the mm-wave phase and the phase shifter in turn influences the amplitude.

V. SPECTROMETER PERFORMANCE

The ESR spectrum of spin-polarized atomic hydrogen shown in Fig. 7 corresponds to the transition from the hyperfine state b to the state c and contains lines originating from the bulk gas in the resonator and the 2D gas adsorbed on the flat mirror. Bulk gas density was $2.1 \times 10^{13} \text{ cm}^{-3}$ and the surface density of the adsorbed atoms $2.5 \times 10^{12} \text{ cm}^{-2}$. The surface line is shifted from the bulk one due to the internal dipolar field created by the 2D gas, and the shift is proportional to the 2D density.¹³ The shape of the bulk line is determined by the inhomogeneity of the main magnetic field. The surface line is broadened due to the inhomogeneity of the internal field caused by the inhomogeneity of the surface density. An ESR excitation power higher than 20 pW may cause an ESR instability in the 2D sample.¹³ The absolute number of atoms in the resonator was calibrated calorimetrically to within 10% by measuring the recombination heat delivered during the decay of the samples. A similar method was used to measure the mm-wave excitation field in the

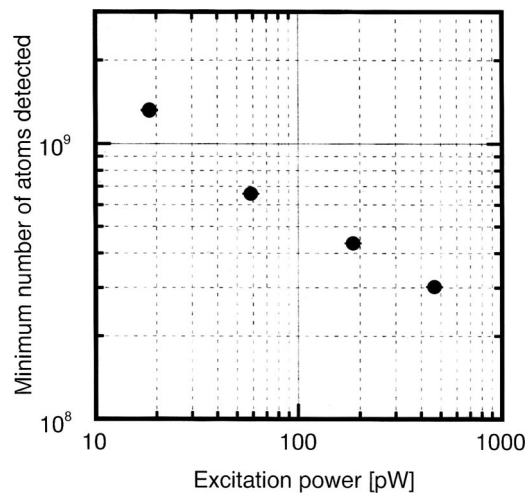


FIG. 8. Sensitivity of the ESR spectrometer measured as a function of the excitation power at a 1 Hz detection bandwidth.

resonator. The ESR signal detected as a change in voltage is proportional to the square root of the excitation power, which is demonstrated in Fig. 8. This dependence was found for the sensitivity of the spectrometer in terms of the number of atoms in the resonator for signal-to-noise (S/N)=1.

To analyze sources of noise, we performed a separate measurement of the main mixer noise at 5 K. The SSB noise temperature of about 200 K was obtained which is a typical value for mixers of this type.⁹ The noise temperature of the preamplifier G_1 was found to be of the same order. When increasing the power of the second IF above 10 μ W, we found that the output noise of the spectrometer starts to grow. In these conditions, balancing the mm-wave bridge reduced the output noise. Fluctuations of the helium vapor density in the oversized waveguide or the internal noise of the SSB generator CM_1 could be reasons for the power dependent noise. Strong drifts of the output signal were observed during transfers of liquid helium into the cryostat supporting the former possibility. At low second IF powers, most of the noise is caused by the main mixer CM_2 and the preamplifier G_1 .

The sensitivity of the spectrometer could be improved by increasing the output power of the mm-wave oscillator. This

would decrease the conversion loss of the main mixer by a couple of dB. The sensitivity at high excitation powers can be increased by mounting the oversized waveguide in a vacuum-tight shield to avoid disturbances due to the helium vapor fluctuations. The noise of the spectrometer at low excitation powers can be reduced by using a cryogenic high electron mobility transistor (HEMT) amplifier with a substantially lower noise temperature than the FET preamplifier used at present.

In conclusion, we have described a sensitive cryogenic heterodyne 128 GHz ESR spectrometer employed in experiments on spin-polarized atomic hydrogen. The spectrometer can detect about 2×10^9 spins/Gauss at a mm-wave excitation power of 20 pW. Absorption and dispersion signals are detected simultaneously.

ACKNOWLEDGMENTS

The authors wish to thank A. I. Safonov for composing software and M. Kemppainen for test measurements of the components. This work was supported by the Academy of Finland, Wihuri Foundation and INTAS. One of the authors (J. J.) thanks the National Graduate School in Materials Physics.

- ¹G. H. van Yperen, I. F. Silvera, J. T. M. Walraven, J. Berkhout, and J. G. Brisson, *Phys. Rev. Lett.* **50**, 53 (1983).
- ²B. W. Statt, W. N. Hardy, A. J. Berlinsky, and E. Klein, *J. Low Temp. Phys.* **61**, 471 (1985).
- ³S. A. Vasilyev, A. Y. Katunin, A. I. Safonov, A. V. Frolov, and E. Tjukanov, *Appl. Magn. Reson.* **3**, 1061 (1992).
- ⁴M. Mertig, E. Tjukanov, S. A. Vasilyev, A. Y. Katunin, and S. Jaakkola, *J. Low Temp. Phys.* **100**, 45 (1995).
- ⁵I. F. Silvera and J. T. M. Walraven, in *Progress in Low-Temperature Physics* (North-Holland/Elsevier, Amsterdam, 1986), Vol. 10, p. 139.
- ⁶A. R. Kerr, *IEEE Trans. Microwave Theory Tech.* **23**, 781 (1975).
- ⁷E. L. Kollberg and H. H. G. Zirath, *IEEE Trans. Microwave Theory Tech.* **31**, 230 (1983).
- ⁸J. W. Archer, *Rev. Sci. Instrum.* **56**, 449 (1985).
- ⁹A. V. Räisänen, Ph.D. thesis (Helsinki University of Technology), 1980.
- ¹⁰Type AA138B3 manufactured by FRISD, Tomsk, Russia; <http://www.niipp.ru/eng/main.html>
- ¹¹P. J. Meier, *IEEE Trans. Microwave Theory Tech.* **22**, 1212 (1974).
- ¹²Manufactured by Ferrite Domen Co., St. Petersburg, Russia; <http://www.domen.ru/products/>
- ¹³S. A. Vasilyev, J. Järvinen, A. I. Safonov, A. A. Kharitonov, I. I. Lukashovich, and S. Jaakkola, *Phys. Rev. Lett.* **89**, 153002 (2002).

Review of Scientific Instruments is copyrighted by the American Institute of Physics (AIP). Redistribution of journal material is subject to the AIP online journal license and/or AIP copyright. For more information, see <http://ojps.aip.org/rsio/rsicr.jsp>
Copyright of Review of Scientific Instruments is the property of American Institute of Physics and its content may not be copied or emailed to multiple sites or posted to a listserv without the copyright holder's express written permission. However, users may print, download, or email articles for individual use.